Research Paper
Journal of Aerospace System Engineering
Vol.13, No.4, pp.10-17 (2019)

ISSN 1976-6300
EISSN 2508-7150
http://dx.doi.org/10.20910/JASE.2019.13.4.10

Effect of delamination on vibration characteristic of smart laminated composite plate

Ganesh Shankar†, Jayant Prakash Varun[a], P.K.Mahato[a]
† Department of Mechanical Engineering, Ramgarh Engineering College Ramgarh, Jharkhand, India,825101
aDepartment of Mechanical Engineering, Indian Institute of Technology(Indian School of Mines), Dhanbad 826004, INDIA

Abstract

This study is concerned with a numerical analysis based on the finite element method to describe the effect of midplane delamination in smart laminated composite plate structures. A new finite element model for centrally located delamination and healthy section was developed and coded in Matlab. The transient analysis of delaminated composite plate with integrated Active Fiber Composite (AFC) was investigated in the present article. The formulation of the governing equation was based on the minimum total potential energy approach. The Newmark time integration technique was employed to solve the differential equations. A parametric study on the effects of boundary conditions and AFC patch location, in presence of delamination on the laminated plate were studied.

Key Words: Delamination, composite, finite element, Active fiber composite

1. Introduction

The use of composite materials in aircraft industries, marine structures and automobile sectors are very common, due to its high strength and stiffness. Composite laminates are usually subjected to external impact load during service, which may result in delamination in case of laminated composite structures or debonding between face sheets and core in case of sandwich structures. The cause of delamination may be either due to imperfect fabrication techniques (air entrapment or residual stresses), or due to fatigue loads during the service period of the structure. Due to delamination in composite structures, structural stiffness degrades. The study of delamination is mainly categorized into two methods, (i) Region wise approach and (ii) Layer wise model approach [1]. Delamination reduces the strength and stiffness of structures [2]. Acharyya et al. [3] have investigated the dynamic behaviour of delaminated composite shallow cylindrical shells in different boundary conditions by using finite element methodology. Noh and Lee [4] have worked on the dynamic stability of delaminated composite skew structures under various periodic in-plane loading conditions, they investigated the behaviour of laminated skew plate structures with various delamination sizes and fiber angle of different layers. Kumar et al. [5] discussed the effect of different kind of delamination and their effect on the second bending and first torsional mode shape. They incorporated the delamination in the Carrera Unified formulation frame work using nine noded quadrilateral MITC9 elements. A meshfree method along with Hamilton system based on the three-dimensional semi-analytical model have developed by Chen et al. [6] for the free vibration of delaminated composite laminates. A linear and nonlinear vibration response of glass fibre reinforced composites with delamination is studied by Hammami et al.[7], an experimental attempt has been made to investigate the effect of delamination size on the

Received: Oct. 13, 2018 Revised: Feb. 04, 2019 Accepted: Feb. 17, 2019
† Corresponding Author
Tel: +91-8609281020, E-mail: GSHANKAR406@gmail.com

linear and nonlinear dynamic behaviour of the composites.

A lot of researches are available on the structural active vibration control by using conventional piezoelectric actuators and sensors. The application based use of piezoelectric actuators as smart structures are presented by Crawley and Luis [8]. Tzou and Tseng [9] have proposed a new structure containing integrated distributed piezoelectric sensor and actuator where the distributed piezoelectric sensing layer monitors the structural oscillation due to direct piezoelectric effect and the distributed actuator layer suppresses the oscillation via the converse piezoelectric effect. Woo-Seok et al. [10] suggested a numerical solution and design strategy for a laminated composite plate with piezoelectric sensors or actuator where the vibration is controlled by passive and active control methods. Active Fiber Composite is a special type of smart material with interdigitated electrode embedded on its surface which was originally developed by Hagood and Bent [11]. It has high value of piezoelectric charge constant Mahato and Maiti [12, 13] investigated flutter control analysis of AFC laminate subjected to hygrothermal environment. Brunner et al. [14] discussed the capability of AFC in structural health monitoring. Guruprasad et al. [15] have modeled the AFC as a sensing device for detecting the damage and delamination in structure. Martinez and Artemev [16] studied the actuation degradation of AFC in presence of fibre damage.

In the present study, the effect of delamination and the effect of active fiber position on the laminated structure are presented. Mathematical formulation is based on finite element method coded in Matlab. The displacement field variable is based on first order shear deformation theory.

2. Mathematical formulations

A laminated plate with 'n' number of layers, whose 1st and Nth layers are AFC actuators and sensors respectively, is shown in Fig.1. The first order shear deformation theory has been incorporated for the analysis. The constitutive equations of Electro-Mechanical [12] relationship are given as follows.

$$\{\sigma_{ij}\}=[Q_{ij}]\{\varepsilon_{ij}\}-[e_{ij}]\{E_i\}$$
$$\{D_i\}=[e_{ij}]\{\varepsilon_{ij}\}+[\kappa]\{E_i\} \quad (1)$$

Where, $\{\sigma_{ij}\}$ is the stress vector $[Q_{ij}]$ is the constitutive matrix, $\{\varepsilon_{ij}\}$ is the strain vector due to mechanical loading, $\{D_i\}$ is the electric displacement, $[e_{ij}]$ is the piezoelectric stress coefficient matrix, $[\kappa]$ is the dielectric constant, $\{E_i\}$ is the electric field vector.

$$E_1=-V/h_e \quad (2)$$

Equation (2) represent the electric field, where V= voltage potential, and h_e denote the space between two electrode which is shown in Fig. 1

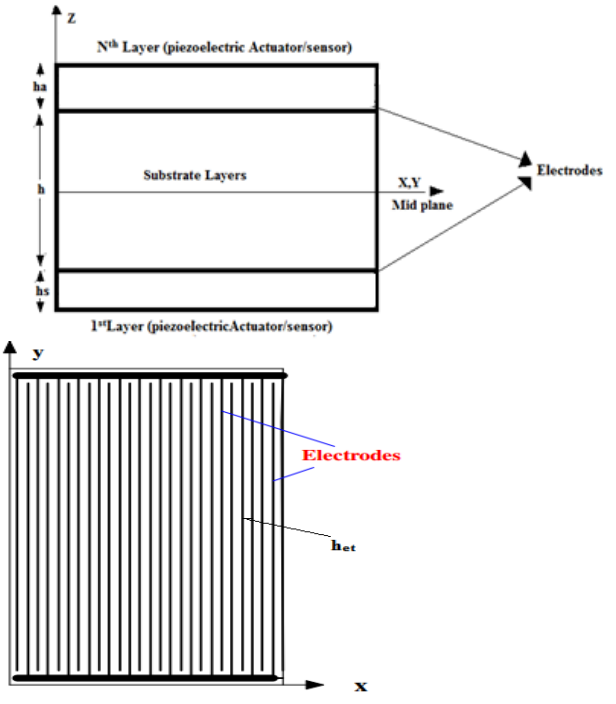

Fig. 1 Laminated plate with Actuator and sensor layer

3. Finite element formulations of healthy plate and delaminated plate

Element for a healthy plate, based on the first order displacement theory is derived through the following process. An eight-noded serendipity element, with five degrees of freedom at each node, is adopted here for the element formulation shown in equation (3). Displacement fields are interpolated by using Lagrangian shape function. Similarly, an element for delaminated segment is meshed separately. Figure. 2. shows the coordinate system of the healthy and delaminated segment of plate.

$$u_0=\sum_{i=1}^{8}N_iu_i \quad , \; v_0=\sum_{i=1}^{8}N_iv_i \quad ,w_0=\sum_{i=1}^{8}N_iw_i$$
$$,\theta_x=\sum_{i=1}^{8}N_i\theta_{x_i} \quad ,\theta_y=\sum_{i=1}^{8}N_i\theta_{y_i} \tag{3}$$

Here *Ni*s shape function. The displacement field of the element is assumed to be the following form relative to its own local coordinate system in equation (4).

$$\begin{aligned} u(X,Y,Z)&=u_0(X,Y)+Z\theta_x(X,Y)\\ v(X,Y,Z)&=v_0(X,Y)+Z\theta_y(X,Y)\\ w(X,Y,Z)&=w_0(X,Y)\end{aligned} \tag{4}$$

Strain displacement relationship is shown in equation 5.

$$\{\varepsilon\}=[B]\{\delta\},\ or\ [B]=\sum_{i=1}^{40}[\partial N_i] \tag{5}$$
$$\{\delta\}=\{u_i,v_i,w_i,\theta_{xi},\theta_{yi},.....\}$$

Here ε is mid-plane normal strain along material coordinate direction and {δ} is deformation at each node. Degree of freedom for each element is 8×5= 40. Each lamina may have different orientations with respect to global or structural co-ordinate system. Hence, a co-ordinate transformation from the material co-ordinate system to the structural co-ordinate system is required. If the lamina is oriented at an angle Θ with respect to the structural/global reference frame, then the in-plane strain transformation matrix is given by Equation 6:

$$\begin{Bmatrix}\varepsilon_X\\ \varepsilon_Y\\ \varepsilon_{XY}\end{Bmatrix}=\begin{bmatrix}m^2 & n^2 & -2mn\\ n^2 & m^2 & 2mn\\ mn & -mn & m^2-n^2\end{bmatrix}\begin{Bmatrix}\varepsilon_{11}\\ \varepsilon_{22}\\ \varepsilon_{12}\end{Bmatrix} \tag{6}$$

Where m=cos Θand n=sin Θ

Once the strains measured in global co-ordinate system are obtained, the stress-resultants can be obtained by integrating the stresses through the thickness of the laminate. The stress resultants due to mechanical loading are given by Equation 7.

$$\begin{Bmatrix}N_x\\ N_y\\ N_{xy}\\ M_x\\ M_y\\ M_{xy}\end{Bmatrix}=\begin{bmatrix}A & B\\ C & D\end{bmatrix}\begin{Bmatrix}\varepsilon_x\\ \varepsilon_y\\ \varepsilon_{xy}\\ k_x\\ k_y\\ k_{xy}\end{Bmatrix}$$

$$[A_{ij}]=\sum_{k=1}^{n}\left[Q_{ij}\right]_k(z_k-z_{k-1})$$
$$[B_{ij}]=\frac{1}{2}\sum_{k=1}^{n}\left[Q_{ij}\right]_k(z^2{}_k-z^2{}_{k-1}) \tag{7}$$
$$[D_{ij}]=\frac{1}{3}\sum_{k=1}^{n}\left[Q_{ij}\right]_k(z^3{}_k-z^3{}_{k-1})$$

Where N_x, N_y, and M_x, M_y are the normal forces and bending moments respectively along X, Y axis where as N_{xy} and M_{xy} are in-plane shear force and twisting moment. [A_{ij}]=extensional stiffness matrix, [B_{ij}] = extension bending coupling matrix, [D_{ij}] =bending stiffness matrix and [Q_{ij}] =transformed, reduced constitutive stiffness matrix of laminae. n= number of layers and 'k' is taken as an arbitrary layer.

In case of delamination the global coordinate systems for the upper and lower sub-laminate are x^l, y^l, z^l. If 'p' is the number of layers in the lower delaminated part and 'n' is the total number of layers, then the bending stiffness matrix and density matrix are changed according to Equation (8).

Lower delamination bending stiffness

$$[a_{ij}]_L=\sum_{k=1}^{p}[Q_{ij}]_k(Z_k-Z_{k-1})$$
$$[b_{ij}]_L=\frac{1}{2}\sum_{k=1}^{p}[Q_{ij}]_k(Z^2{}_k-Z^2{}_{k-1})$$
$$[d_{ij}]_L=\frac{1}{3}\sum_{k=1}^{p}[Q_{ij}]_k(Z^3{}_k-Z^3{}_{k-1})$$

Upper delamination bending stiffness

$$[a_{ij}]_U=\sum_{k=p+1}^{n}[Q_{ij}]_k(Z_k-Z_{k-1})$$
$$[b_{ij}]_U=\frac{1}{2}\sum_{k=p+1}^{n}[Q_{ij}]_k(Z^2{}_k-Z^2{}_{k-1}) \tag{8}$$
$$[d_{ij}]_U=\frac{1}{3}\sum_{k=p+1}^{n}[Q_{ij}]_k(Z^3{}_k-Z^3{}_{k-1})$$

Now stiffness and mass matrices of the element can be derived by equation (9)

$$[K^e]=\int_{-1}^{1}\int_{-1}^{1}[B]^T\overset{*}{[D]}[B]dxdy \quad [m^e]$$
$$=\int_{-1}^{1}\int_{-1}^{1}[F]^T[\rho^k][F]dxdy \tag{9}$$

Now assemble the stiffness and mass matrices for the entire element globally then the global stiffness and mass matrices are [K] and [M].

The kinetic energy of delaminated and healthy plate element and the total potential energy due to mecha nical, electrical, mechanical external load and AFC (p iezo-fiber) external load is given below.

$$T_p = \frac{1}{2}\sum_{L=2}^{N-1}\int_{\Omega}\{\varepsilon^L\}^T\{\sigma^L\}d\Omega + \frac{1}{2}\int_{\Omega}\{\varepsilon^1\}^T\{\sigma^1\}d\Omega - \frac{1}{2}\int_{\Omega}\{E^1\}^T\{D^1\}d\Omega - \frac{1}{2}\int_{\Omega}\{\varepsilon^n\}^T\{\sigma^n\}d\Omega - \frac{1}{2}\int_{\Omega}\{E^n\}^T\{D^n\}d\Omega - \int_A\{\delta\}^T\{q\}dA - \int_{A(z=h_n)}V\psi(x,y)dA$$

$$T_{KE} = \frac{1}{2}\sum_{K=1}^{N}\int_A\{\dot{\delta}^T\}[m]\{\dot{\delta}\}dA \quad (10)$$

Here T_p and $T_{KE}$are the total potential energy and kinetic energy of the laminate; Ω stand for volume of the element and A stands for area of the element, $\psi(x,y)$ is surface charge density at the actuator layer, N denotes number of layer of laminate which is actuator/sensor, other symbols having same meaning which have describe above sections. Now applying the principle of minimum energy approach and substituting above equation in equation (10) we get three set of equilibrium equations with respect to a nodal variable which is given as:

$$\begin{aligned}&[M^e]\{\ddot{\delta}^e\}+[K^e_{dd}]\{\delta^e\}-[K^e_{da}]\{V^{en}\}\\&-[K^e_{ds}]\{V^{e1}\}=\{F^e_1\}\\&[K^e_{ad}]\{\delta^e\}+[K^e_{aa}]\{V^{en}\}=\{F^e_2\}\\&[K^e_{sd}]\{\delta^e\}+[K^e_{ss}]\{V^{e1}\}=\{0\}\end{aligned} \quad (11)$$

Where $[M^e]$ is the elemental mass matrix and $[k^e_{dd}]$, $[k^e_{aa}]$ and $[k^e_{ss}]$ are the elemental stiffness matrices due to mechanical displacements, the actuators and sensors potential respectively. $[k^e_{da}]$ and $[k^e_{ds}]$ are the electromechanical coupling stiffness matrices where subscript 'a' for actuator and 's' for the sensor is adopted. $\{F^e_1\}$ and $\{F^e_2\}$ are elemental mechanical force vector and elemental electrical force vector respectively. $\{V^{e1}\}$ and $\{V^{en}\}$ are the voltages induced at first and last layer of the laminate. $\{\delta^e\}$ denote the elemental deformation vector due to mechanical or electrical loading. Now the global equilibrium equations are obtained after the assembling the equation (11) with respect to the global axis.

$$\begin{aligned}&[M\ ]\{\ddot{X}\}+[K_{dd}]\{X\}-[K_{da}]\{V_a\}\\&-[K_{ds}]\{V_s\}=\{F_1\}\\&[K_{ad}]\{X\}+[K_{aa}]\{V_a\}=\{F_2\}\\&[K_{sd}]\{X\}+[K_{ss}]\{Vs\}=\{0\}\end{aligned} \quad (12)$$

Where $[M]$ is the global mass matrices and $[K_{dd}]$, $[K_{aa}]$, $[K_{ss}]$, $[K_{da}]$, $[K_{ds}]$, $[K_{ad}]$, $[K_{sd}]$ are the global generalized stiffness matrices $\{X\}$ is the global displacement vector and $\{F_1\}$ is the mechanical force vector, $\{F_2\}$ is the electric force vector. Eliminating $\{V_a\}$ and $\{V_s\}$ in Equation (12) can be rewritten as:

$$[M]\{\ddot{X}\}+[K^*]\{X\}=\{F_1\}+\{F_c\} \quad (13)$$

Where, $[K^*]$ and $\{Fc\}$ are the controlling stiffness a nd control feedback force. The detail control mechan ism is given in Mahato and Maiti [12]. Differential eq uations are solved by Newmark integration technique [17].

$$\begin{aligned}&[K^*]=[K_{dd}]+[K_{da}][K_{aa}]^{-1}[K_{ad}]+\\&[K_{ds}][K_{ss}]^{-1}[K_{sd}]\\&\{F_c\}=[K_{da}][K_{aa}]^{-1}\{F_2\}\end{aligned} \quad (14)$$

4. Result and discussion

Numerical results are presented in this section is based on finite element code developed in MATLAB. The AFC patches are integrated at the top and bottom of the plate. Electro-Mechanics is also incorporated into the finite element code developed for the AFC patches. A parametric study on the effect of AFC patch location, with midplane delamination and various boundary conditions is carried out. The material properties of graphite/epoxy and AFC (piezoelectric) layer are shown in Table 1.

An asymmetric laminated square plate of dimension $0.6m\times0.6m\times0.006m$ and orientation of each ply is (90/0/90/0) is taken for the analysis. A square delamination size $0.3m\times0.3m$ (25% of the total area) is present in middle of the laminate. Space between two electrodes is $0.00025m$. The plate is divided into 8×8 mesh element. The analysis is carried out for three different boundary conditions i.e. all edges are

simply supported (S-S-S-S), cantilever boundary condition (C-F-F-F) and clamped-clamped boundary condition (C-C-C-C), here 'C' stand for clamped edge 'F' for free edge and 'S' for simply support edge. A point load of $1000N$ is applied at the middle of the plate (middle node) in case of S-S-S-S and C-C-C-C boundary condition and at midpoint of free end in C-F-F-F boundary condition for initial excitation. Figure 2 shows the geometry of the plate and delamination location within the plate.

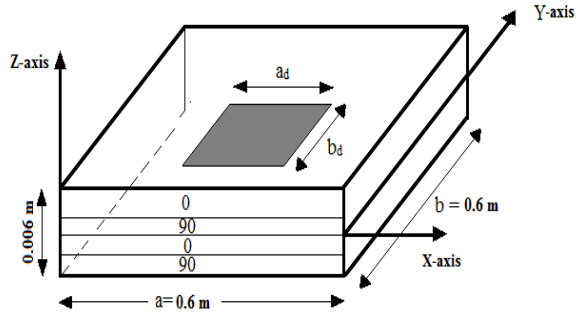

Figure.2 Plate geometry and delamination location

Figure 3. shows the AFC patches position at different location on both side of plate. Here, four different location of patches position is discussed for the dynamics analysis
of delaminated composite plate. Size of one AFC patches which is shown in Figure 3 (a), 3 (b), and 3(c) is $0.15m \times 0.15m$. In Figure 3(d) AFC patch size is taken $0.3m \times 0.3m$ which is exactly same as delamination size.

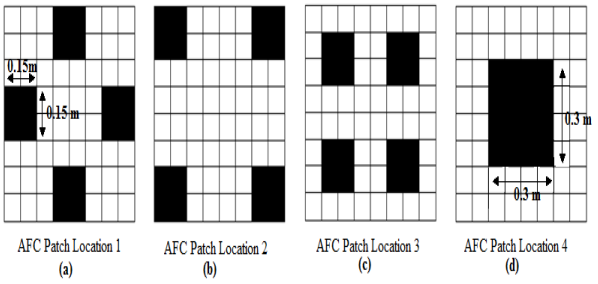

Fig. 3AFC patches location at different places on plate

Table 1 Material properties of graphite/epoxy and AFC - 50% fiber volume fraction.

Elastic module	graphite/epoxy [12]	AFC layer [12]
E_{11} (Gpa)	128	119.7
E_{22} (Gpa)	6.12	129.1
μ_{12}	0.3	0.35
μ_{13}	---	0.38
G_{12} (Gpa)	5.0	39.14
G_{13} (Gpa)	5.0	32.35
G_{23} (Gpa)	2.5	32.35
$e_{11}(c/m^2)$	---	14.14
$e_{21}(c/m^2)$	---	-3.34
$e_{24}(c/m^2)$	---	10.79
κ_{11}(F/m)	---	8.599×10^{-9}
κ_{33}(F/m)	---	6.485×10^{-9}
Density (Kg/m^3)	1600	6700

4.1 The effect of delaminations and AFC patches positions in terms of Transient analysis.

Transient analysis of delaminated plate with AFC patches is studied in this section. A point load of $1000N$ is applied at middle of the plate in simply supported and clamped-clamped boundary, whereas it will be act at midpoint of free end in case of cantilever boundary condition. After giving an initial displacement, the load is suddenly removed and the plate is kept at vibration. A feedback system is activated at the mean time. The output voltage of the sensor layer is amplified by the amplifier and feedback to the actuator layer. Effective damping is produces by AFC patches which diminish the dynamic responses.

Figure 4 shows the significant change in dynamic displacement response due to AFC patches position with respect to time history in S-S-S-S boundary condition. The velocity feedback gain is taken 1(G_v=1), and voltage applied at actuator layer is 0.001 volt. Dynamic response is recorded for 0.5 second. In delaminated condition maximum amplitude is $0.0121m$, $0.0092m$, $0.009m$ and $0.0033m$ when AFC patch location 1, 2, 3 and 4 respectively whereas in without delamination maximum amplitude is recorded $0.0052m$, $0.0043m$, $0.0041m$ and $0.0027m$ at patch location 1, 2, 3 and 4 respectively. So it is clear from available data that delaminated structures dynamic displacement amplitude is more than without delaminated plate structure. Maximum dynamic displacement is obtained in case of AFC patch position 1 and least amplitude is obtained at AFC patches location 4 in S-S-S-S boundary

condition.

Figure. 5 shows the time versus dynamic displacement response in C-F-F-F boundary condition for various AFC patch position as discuss in Figure 3.The velocity feedback gain is kept on 1(G_v=1), and voltage applied at actuator layer is 0.001 volt. Dynamic response is recorded for 0.5 second. The amplitude of delaminated plate is more than without delaminated plate structure when AFC patch position 1, 2 and 3 shown in Figure 5(a), 5(b) and 5(c) whereas it is nearly equal amplitude from delamination to without delamination at AFC patch position 4 clearly shown in Figure 5(d). Maximum amplitude in without delaminated plate is 0.0840m, 0.09011m, 0.08793m and 0.094174 corresponding to AFC patch position 1, 2, 3 and 4 respectively where as in delaminated condition maximum amplitude is increased by 31 %, 24.65%, 24.23% and 4% corresponding to AFC patch position 1, 2, 3 and 4 respectively in C-F-F-F boundary condition.

In clamped-clamped boundary condition dynamic displacement response in varying time history is shown in Figure. 6. In this boundary condition maximum amplitude in delaminated case is recorded at AFC patch position 2 whereas minimum occur at AFC patch position 4. Detail analysis of dynamic displacement versus time is shown in Figure 6 (a), 6 (b), 6(c) and 6(d).

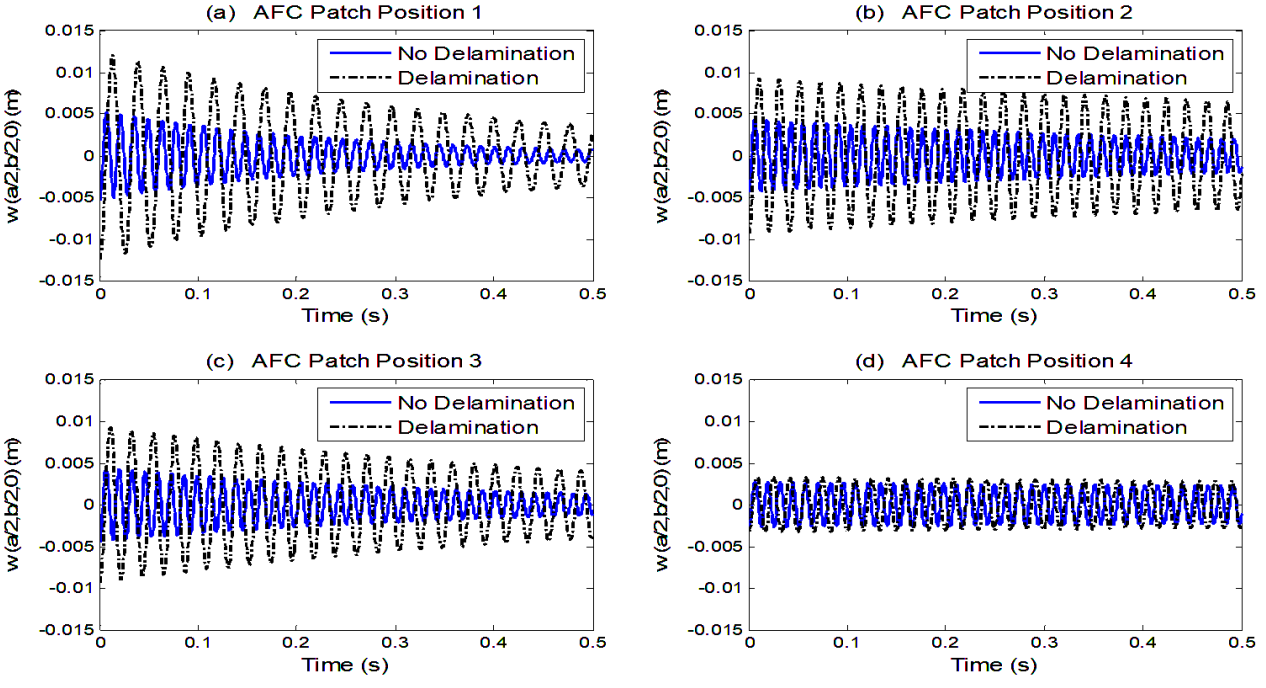

Fig. 4. Time response of delaminated and without delaminated plate at different location of AFC patches (Gv=1) in S-S-S-S boundary condition.

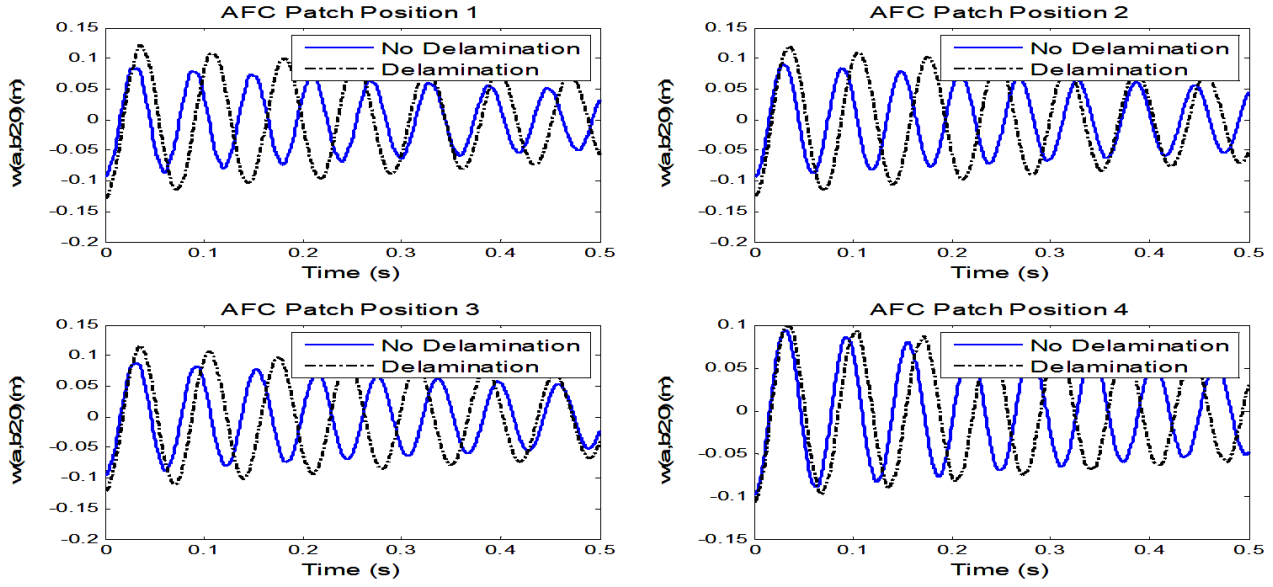

Fig. 5. Time response of delaminated and without delaminated plate at different location of AFC patches (Gv=1) in C-F-F-F boundary condition

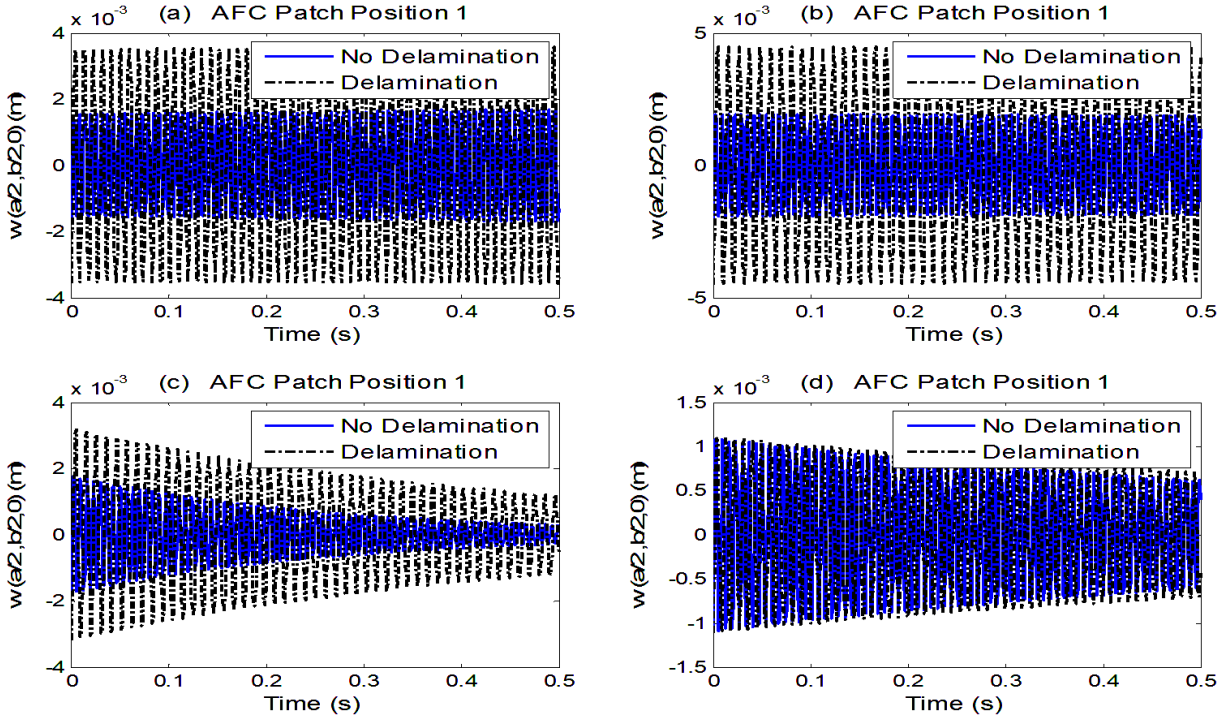

Fig. 6. Time response of delaminated and without delaminated plate at different location of AFC patches (Gv=1) in C-C-C-C boundary condition.

4. Conclusions

A Matlab based finite element code is developed for the control analysis of delaminated composite plates including AFC actuators/sensors and feedback control loop. The transverse displacement has been deduced in time frame. It is observed that the dynamic responses amplitude is larger in the case of

delamination. It is also observed that significant changes are occurred due to various boundary conditions and AFC patches positions, when patches are near to delaminated region is good for structural control and having less dynamic displacement

References

[1] C.N. Della, D. Shu, Vibration of delaminated composite laminates: A review, Appl. Mech. Revie. 60, 1-20 ,2007.

[2] F. Ju, H.P. Lee, K.H. Lee, Finite element analysis of free vibration of delaminated composite plates, Compos. Eng.5 195-209, 1995.

[3] A. K. Acharyya, D. Chakravorty, & A. Karmakar, Natural frequencies and mode shapes of composite cylindrical delaminated shells by finite element. *Journal of Reinforced Plastics and Composites*, *29*(2), 226-237 2010.

[4] M. H. Noh, S. Y. Lee, Dynamic instability of delaminated composite skew plates subjected to combined static and dynamic loads based on HSDT. *Composites Part B: Engineering*, *58*, 113-121 2014.

[5] S. K. Kumar, M. Cinefra, E.Carrera, R. Ganguli, D. Harursampath, Finite element analysis of free vibration of the delaminated composite plate with variable kinematic multilayered plate elements. *Composites Part B: Engineering*, *66*, 453-465 2014.

[6] J. Chen, H. Wang, G. Qing, Modeling vibration behavior of delaminated composite laminates using meshfree method in Hamilton system. *Applied Mathematics and Mechanics*, *36*(5), 633-654 2015.

[7] M. Hammami, A. El Mahi, C. Karra, M. Haddar, Experimental analysis of the linear and nonlinear behaviour of composites with delaminations. *Applied Acoustics*, *108*, 31-39 2016.

[8] E.F. Crawley, J. De Luis, Use of piezoelectric actuators as elements of intelligent structures, AIAA J. 25 (1987) 1373-1385.

[9] H.S Tzou, C.I. Tseng, Distributed piezoelectric sensor/actuator design for dynamic measurement/control of distributed parameter systems: a piezoelectric finite element approach. Journal of sound and vibration **138(1)** :17-34, 1990.

[10] W.S. Hwang, W. Hwang, H.C Park, Vibration control of laminated composite plate with piezoelectric sensor/actuator: active and passive control methods. Mechanical Systems and Signal Processing **8(5):**571-83, 1994.

[11] N.W. Hagood, A.A. Bent, Development of piezoelectric fiber composites for structural actuation. AIAA/ASME/ASCE/AHS/ASC 34th Struct. Dynamics and Mater. Conference 3625-3638, 1993.

[12] P.K. Mahato, D.K. Maiti, Aeroelastic analysis of smart composite structures in hygro-thermal environment. Compos. Struct. 92 :1027-1038, 2010.

[13] P.K.Mahato, D.K. Maiti, Flutter control of smart composite structures in hygrothermal environment, J. Aerospace Eng. **23**: 317-326, 2010.

[14] A.J. Brunner, M. Barbezat, C. Huber, P.H. Flüeler, The potential of active fiber composites made from piezoelectric fibers for actuating and sensing applications in structural health monitoring. Mater. and struct**38**: 561-567, 2005.

[15] P.J.Guruprasad, A.K Tamrakar, D. Harursampath, Modeling of active fiber composite for delamination sensing. Smart Mater. Nano-and Micro-Smart Syst. 641305-641305, 2006.

[16] M. Martinez, A. Artemev, Finite element analysis of broken fiber effects on the performance of active fiber composites. Compos. Struct. **88** :491-496, 2009.

[17] Bathe KJ, Wilson EL. Numerical methods in finite element analysis. Englewood Cliffs, NJ: Prentice-Hall; 1976.